Surface damage of W exposed to combined stationary D plasma and ELMs-like pulsed plasma

Y.Z. Jia[1, 2, *], W. Liu[2,**] , B. Xu[2], S.L. Qu[2], T.W. Morgan[3]

[1] *Science and Technology on Reactor Fuel and Materials Laboratory, Nuclear Power Institute of China, Chengdu, Sichuan 610213, China.*

[2] *Laboratory of Advanced Materials, School of Materials Science and Engineering, Tsinghua University, Beijing 100084, China.*

[3] *FOM Institute DIFFER-Dutch Institute for Fundamental Energy Research, 5612AJ Eindhoven, The Netherlands.*

* Corresponding author. Tel.: +86 18382112384; E-mail address: jaja880816@aliyun.com.

** Corresponding author. Tel.: +86 01062772852; E-mail address: liuw@mail.tsinghua.edu.cn.

Abstract

The surface damage of W under D plasma and ELMs-like transient heat loads was studied by combined stationary and pulsed D plasma. Low-flux transient heat loads will promote blister formation due to the gas expansion inside the blisters. On the contrary, high-flux transient heat loads will mitigate blistering due to the high surface temperature. Therefore, blistering on W surface first increased and then decreased with the increasing transient heat loads. The promotion effect of pulsed plasma on blistering is more obvious on [001] and [110] surfaces than on [111] surface, and the orientation dependence of blisters was mitigated by the transient heat loads. Surface modification induced by transient heat loads only formed on [001] and [110] surfaces, but did not form on [111] surface. The orientation dependence of surface modification was mainly due to the slipping system of dislocations.

1. Introduction

Due to its favorable physical properties, such as low sputtering yield, high melting temperature and high thermal conductivity, tungsten (W) will be used as a plasma facing material (PFM) in the ITER divertor [1, 2]. As a PFM, W will be subjected to the transient heat loads of Edge Localized Modes (ELMs), the number of which will be higher than 10^6 events during the lifetime of divertor [3].

Previous studies have shown that the transient heat loads of ELMs will induce surface damage, such as surface modifications, cracking and melting of W surfaces [4-6]. Besides the transient heat loads, W will simultaneously be subjected to high fluxes and fluences of stationary plasma ions (D, T, He), of which D and T are the main plasma species. D plasma will also induce some types of surface damage, for example, strong blistering [7-9] and some other surface morphology [10-12] on W surface. The occurrence of these ELMs-induced and D-induced surface damage is significant threat to the lifetime of divertor and its compatibility with high plasma performances.

Therefore, it is important to study the surface damage behavior of W material under combined D plasma and ELMs-like transient heat loads condition. Many studies have been carried out in this field in recent years [13-21], but experimental conditions were different in each study, and were also not same as the working condition of divertor in ITER. For instance, in some studies, W samples were sequentially (not simultaneously) exposed to D plasma and transient heat loads [13, 14, 19-21]; in some other studies, ELMs-like heat loads were simulated by laser beam [13-18] or electron beam [19, 20], but ELMs were transient plasma events in ITER. Therefore, the surface damage of W under combined steady state D plasma and ELMs-like transient heat loads still needs more research.

In this study, W samples were exposed to combined stationary D plasma and ELMs-like pulsed plasma simultaneously, and the surface damage caused by the exposure was studied in detail. The conditions of stationary D plasma and pulsed plasma are similar to the stationary plasma and ELMs heat loads in ITER. Therefore, the results of present study will shed new light on the surface damage of W under working conditions of PFMs.

2. Experimental

Polycrystalline W samples with purity of 99.95 wt% were cut from a rolled sheet, which was supplied by Advanced Technology & Materials CO., Ltd. (China). The main impurities are Mo, Fe, O with concentrations below 15 wppm, and C with a concentration around 50 wppm. All the samples were stress relieved at 1273 K at a background pressure of 5×10^{-4} Pa for 1 hour after polishing and before implantation. All samples were exposed to combined steady-state and pulsed D plasma in Pilot-PSI linear plasma generator using the pulsed plasma system described in [18, 21-23]. The time evolution of the surface temperature during the exposure was monitored by a fast infrared camera (FLIR SC7500MB) with a frame rate around 3 kHz. The evolution of the peak temperature during a shot is shown in Fig.1 (a). The base temperature (*BT*) was caused by the steady heat flux of the stationary plasma, and the temperature rise (ΔT) was caused by the plasma pulses. During a shot, the steady-state plasma duration was 10 s, and the plasma pulses were triggered for 5 s with a frequency 10 Hz (50 plasma pulses). The details of the plasma pulses can be found in reference [21]. For each sample, the same shot was repeated for 10 times, so the accumulated number of plasma pulses was 500. Fig.1 (b) shows the distribution of surface temperature and heat flux density during the exposure of stationary plasma and pulsed plasma. The target heat fluxes were calculated using the THEODOR code [24], a 2D inverse heat transfer code. On the same sample, in the center area (radius ≤ 7 mm), the *BT* was almost the same, but ΔT varied a lot at different positions. The highest ΔT was about 700 K, and the corresponding transient heat flux of the plasma pulse was about 300 MW/m^2. In this study, for different samples, the *BT* of surface was set at 650 K or 800 K, and ΔT varied from 200 K to 700 K.

The conditions of the stationary plasma during the exposure were listed in Table.1. The flux of stationary D plasma was about 1×10^{24} m^{-2}s^{-1}, and the ion energy was controlled by negatively biasing the sample and was fixed to ~38 eV. The plasma conditions were kept constant throughout this study. For each sample, the total fluence of D plasma during 10 shots was about 1×10^{26} m^{-2}.

The surface morphology changes of the samples were observed using a TESCAN MIRA 3 LMH high-resolution scanning electron microscope (SEM). The crystallographic grain orientation was analyzed by Oxford instrument NordlysMax^2 electron backscatter diffraction technique (EBSD).

3. Results

3.1 Surface morphology at *BT* = 650 K

Fig.2 shows the surface morphology of samples exposed to stationary/pulsed plasma with BT = 650 K and different ΔT. After the exposure, two main types of surface damage morphology formed on the surface: blisters induced by D plasma and surface modification caused by the transient heat loads of plasma pulses. When ΔT was low, the blisters only formed on parts of the surface, but when ΔT reached 500 K, the whole surface was covered with blisters. When ΔT > 500 K, the blister density decreased with the increasing ΔT, and when ΔT = 700 K, no blisters formed on the surface. For the surface modification, only when ΔT ≥ 600 K, the modification morphology can be observed on the exposure surface. The D-induced blistering and heat-induced surface modification on W surface is closely dependent on the surface orientation [7, 8, 25-27], so the surface morphology of different surfaces exposed to stationary/pulsed plasma was analyzed respectively. Fig.3 shows the surface morphology of [001] surface, [110] surface and [111] surface with different ΔT. In each image, the deviations of the surface normal directions from [001], [110] or [111] direction are smaller than 5°. The blister coverage on [001], [110] and [111] surfaces with different ΔT were analyzed as shown in Fig.4. The blister coverage was calculated by the ratio of blistered area to the grain surface area. On all three kinds of surfaces, the blisters first increased and then decreased with the increasing ΔT. When ΔT = 320 K, the orientation dependence of blisters is still obvious – blistering is most severe on [111] surfaces and slight on [001] and [110] surfaces, which is similar to the results reported in previous study without transient heat loads [7, 8, 25, 26]. The transient heat loads of plasma pulses increased the blisters density on [001] and [110] surfaces dramatically, so when ΔT = 500 K, the orientation dependence of blisters was less obvious.

Fig.3 also shows that only when ΔT ≥ 600 K, surface modification were observed on [001] and [111] surfaces, as shown in Fig.3 (d) and Fig.3 (h), while no surface modifications were observed on [111] surface even with ΔT = 700 K, as shown in Fig.3 (l).

When ΔT = 500 K, after the exposure to stationary/pulsed plasma, many tiny cracks were formed on [110] surface and aligned on the same direction, as shown in Fig.3 (g). This kind of tiny cracks was also observed on other surfaces with certain surface normal directions, as shown in Fig.5 (a) and (c). In addition, the cracks in Fig.3 (g), Fig.5 (a) and Fig.5 (c) were all perpendicular to the [001] directions of the grains. The cross-section morphology (Fig.5 (b) and (d)) across the black lines in Fig.5 (a) and (c) were obtained by Focused Ion Beam (FIB) and SEM. Many voids formed in the grain beneath the surface, so the effect of grain boundaries on blister formation is not clear in this study. It is shown that some voids were elongated in the direction perpendicular to the surface. Some of the voids intersected with the surface, inducing tiny cracks on the surface, as pointed by the red arrows. According to these results, the mechanism for the tiny cracks was summarized by the schematic diagram in Fig.5 (e). The plasma exposure will induce bubbles elongated parallel or perpendicular to the surface. The bubbles parallel to the surface will induce plastic deformation and blisters on the surface [7-9]. Other bubbles grew perpendicularly to the surface and [001] direction of the grain. When these bubbles intersect with the surface, tiny cracks perpendicular to [001] directions will form on the surface. This kind of cracks was rarely observed in the previous study of W exposed to stationary D plasma alone without transient heat loads [7, 8, 11]. These cracks may be formed due to the heterogeneous stress field and D atoms distribution in the near surface region under the transient heat loads condition.

3.2 Surface morphology at BT = 800 K

Fig.6 shows the surface morphology of samples exposed to stationary/pulsed D plasma with BT = 800 K and different ΔT. Compared to the surface morphology with BT = 650 K (Fig.2), the blistering was much more slight, but it also first increased and then decreased with the increasing ΔT. When $\Delta T \geq 400$ K, almost no blisters were observed on the surface. As for the surface modification, only at $\Delta T \geq 550$ K the transient heat loads induced obvious modification on the surface, as shown in Fig.6 (e) and Fig.6 (f).

Also, the surface morphology of [001], [110] and [111] surfaces with different

ΔT was analyzed in detail, as shown in Fig.7. The blister coverage on [001], [110] and [111] surfaces with different ΔT were analyzed as shown in Fig.8. When BT = 800 K, on [001], [110] and [111] surfaces, the blister coverage first increased and then decreased with the increasing ΔT. Also, the orientation dependence of blisters was mitigated by the transient heat loads, compared to the results without transient heat loads [7].

Fig.7 also shows that when $\Delta T \geq 550$ K, pulsed plasma will induce obvious surface modification on [001] and [110] surfaces, and the surface modification was even more severe when ΔT = 700 K, as shown in Fig.7 (d) and (h). On contrast, no surface modification was observed on [111] surface even with ΔT = 700 K, as shown in Fig.7 (l).

4. Discussion

4.1 The effect of transient heat loads on blistering

From the results described above, no matter at BT = 650 K or 800 K, the blister coverage first increased and then decreased with the increasing ΔT. In our previous study, it was found that the transient heat loads of plasma pulses will make the D_2 gas expand inside the blisters and induce the growth of blisters [21]. Therefore, in this study when ΔT is low, the blister coverage will increase with the increasing ΔT. However, when the transient heat load of plasma pulses or ΔT is higher, the high surface temperature will increase D atoms' releasing rate from the surface and diffusing rate into the matrix, which will reduce the D retention in the near surface region [7, 28, 29], and result in the reduction of blisters with the increasing ΔT.

Therefore, the transient heat loads of pulsed plasma may have different effects on blistering induced by D plasma on two opposite aspects. On one hand, the transient heat loads will cause the expansion of the gas inside the blisters, and make the blistering more severe. On the other hand, the high temperature caused by the transient heat loads will reduce the D retention in the near surface region, and reduce the blisters on the surface. Therefore, with the increasing ΔT, the blisters will first increase and then decrease, till they disappear on the surface eventually.

Blisters induced by D plasma showed strong dependence on surface orientation of W materials at different temperatures in previous study [7, 8, 25, 26]. Blisters tend to form on [111] surfaces, and blisters are rarely observed on [001] and [110] surfaces [7, 8, 25, 26]. It was found that the orientation dependence is due to the differences of plastic deformation of different surfaces [8]. On [111] surfaces, the bubbles beneath the surface can deform the surface layer easily, so more blisters form on [111] surface, but on [001] and [110] surfaces, the bubbles can hardly deform the surface layer, resulting in fewer blisters on [001] and [110] surfaces. In this study, when D-induced bubbles under [001] and [110] surfaces were subjected to transient heat loads of plasma pulses simultaneously, the gas inside the bubbles will expand due to the high temperature, so the gas pressure inside the bubbles can also deform the surface layer of [001] and [110] surfaces. Therefore, when ΔT increased to 500 K, the blister coverage on [001], [110] and [111] surfaces were almost the same. This means the orientation dependence of D-induced blisters was weakened by the transient heat loads.

4.2 The effect of transient heat loads on surface modification

The surface modification induced by the transient heat loads of pulsed plasma was summarized in Fig.9 at different BT and ΔT. No matter at BT = 650 K or 800 K, the lowest ΔT when surface modification formed on the surface was about 550 K - 600 K. In previous study, it was found that the condition when surface modification occurs is closely related to the heat flux density of the electron beam – only when the heat flux density was above 200 MW/m^2 [4, 5], surface modification could be observed on the surface. In present study, ΔT is directly related to the transient heat loads of the pulsed plasma, as shown by the results of THEODOR in Fig.1 (b). When ΔT = 550 K, the corresponding heat flux density is about 230 MW/m^2, which is similar to the heat flux threshold of surface modification obtained in previous study.

In previous study, it was found that transient heat loads will induce modifications on W surface, because the high heat flux will cause strong stress in the near surface region, and the stress will be relaxed by plastic deformation of near surface region, inducing deformation traces on the surface [27]. In Fig.3

and Fig.7, no matter BT = 650 K or 800 K, surface modification only occurred on [001] and [110] surfaces, but not on [111] surfaces. This result is consistent with the results reported in reference [30]. The stress induced by the transient heat loads was mainly compression stress parallel to the surface. The stress will be relaxed by the slipping of dislocation along the slipping directions ([111] directions in W [31]) in the near surface region. When [111] direction is perpendicular to the surface ([111] surface), the compression stress parallel to the surface cannot force the dislocations to slip along [111] directions, so no slipping traces will be observed on [111] surfaces. Therefore, the surface modification induced by pulsed plasma is not observed on [111] surfaces.

4.3 The effect of transient heat loads on cracks

In this study, only when BT = 650 K and $\Delta T \geq 500$ K, obvious cracks will be observed on the surface, as shown in Fig.10 (a), and the cracks mainly occurred along the grain boundaries. When BT = 650 K and $\Delta T < 500$ K, or BT = 800 K, such cracks will not be observed on the surface. The transient heat loads will lead to the expansion of surface material, resulting in the plastic deformation of the surface. After the plasma pulses, the surface will be subjected to huge tensile stress parallel to the surface due to the shrinking of the surface, resulting in cracks along the grain boundaries of W [5]. The cracks formation is closely related BT and heat flux density. Compared to other metals, the ductile-brittle transition temperature (DBTT) of W is high (about 400 K -700 K [32]), and below DBTT, W materials exhibit brittle features. When the BT was below DBTT, the remaining stress caused by transient heat loads will induce violent deformation and brittle cracks. On contrast, when the BT was above DBTT, the stress can be relaxed by plastic deformation. Also, when the transient heat loads is not high enough, the stress will not induce huge deformation of the surface, so cracks will not form either. Therefore, only when BT = 650 K and $\Delta T \geq 500$ K, the transient heat loads of pulsed plasma will cause obvious cracks on the surface.

5. Conclusion

In this study, the surface damage of W exposed to D plasma and ELMs transient heat loads was investigated by stationary and pulsed D plasma. It was found that the transient heat loads may have promotion and inhibition effect on the formation of blisters. The low-flux transient heat loads will promote the blister formation due to the gas expansion inside the blisters. On the contrary, high-flux transient heat loads will mitigate the formation of blisters. Therefore, on W surface exposed to steady-state and pulsed D plasma, blistering first increased and then decreased, with the increasing transient heat loads.

The promotion effect of transient heat loads on blisters formation is more obvious on [001] surface and [110] surface than on [111] surfaces, so the orientation dependence of blisters was weakened by the transient heat loads. This mainly because transient heat loads will lead to the expansion of the bubbles beneath the surface and deform the surface layers of all surfaces, so more blisters will be formed on [001] surface and [110] surface exposed to stationary/pulsed plasma, compared to exposed to stationary plasma alone.

Surface modification induced by transient heat loads only occurred when transient heat flux was high enough, and it was only observed on [001] and [110] surfaces, but not observed on [111] surfaces. The surface modification is the slipping traces of dislocations in near surface region due to the stress induced by the transient heat loads. The orientation dependence of surface modification was mainly due to the orientation dependence of dislocation slipping in W.

Acknowledgement

This work was supported by National Magnetic Confinement Fusion Science Program of China under Grant 2013GB109004, 2014GB117000, and the National Nature Science Foundation of China under Contract No. 51471092.

References:

[1]R. A. Pitts, S. Carpentier, F. Escourbiac, et al., *J Nucl Mater* **438S** (2013) S48-S56.
[2]T. Hirai, F. Escourbiac, S. Carpentier-Chouchana, et al., *Phys Scripta* **T159** (2014) 014006.
[3]A. Loarte, G. Saibene, R. Sartori, et al., *Phys Scripta* **T128** (2007) 222.
[4]T. Hirai, G. Pintsuk, J. Linke, et al., *J Nucl Mater* **390-91** (2009) 751.
[5]J. Linke, T. Loewenhoff, V. Massaut, et al., *Nucl Fusion* **51** (2011) 073017.
[6]Y. Yuan, H. Greuner, B. Boeswirth, et al., *J Nucl Mater* **438S** (2013) S229-S232.
[7]Y. Z. Jia, G. De Temmerman, G. N. Luo, et al., *J Nucl Mater* **457** (2015) 213-219.

[8]Y. Z. Jia, W. Liu, B. Xu, et al., *J Nucl Mater* **477** (2016) 165-171.
[9]W. M. Shu, *Appl Phys Lett* **92** (2008) 21190421.
[10]Y. Z. Jia, W. Liu, B. Xu, et al., *J Nucl Mater* **463** (2015) 312-315.
[11]M. H. J. 't Hoen, M. Balden, A. Manhard, et al., *Nucl Fusion* **54** (2014) 083014.
[12]H. Y. Xu, Y. B. Zhang, Y. Yuan, et al., *J Nucl Mater* **443** (2013) 452-457.
[13]S. Kajita, D. Nishijima, N. Ohno, et al., *J Appl Phys* **100** (2006) 10330410.
[14]S. Kajita, N. Ohno, S. Takamura, et al., *Appl Phys Lett* **91** (2007) 26150126.
[15]K. R. Umstadter, R. Doerner, G. Tynan, *J Nucl Mater* **386-88** (2009) 751-755.
[16]K. R. Umstadter, R. Doerner, G. R. Tynan, *Nucl Fusion* **51** (2011) 0530145.
[17]G. G. van Eden, T. W. Morgan, H. J. van der Meiden, et al., *Nucl Fusion* **54** (2014) 12301012.
[18]M. Wirtz, S. Bardin, A. Huber, et al., *Nucl Fusion* **55** (2015) 12301712.
[19]M. Wirtz, J. Linke, G. Pintsuk, et al., *J Nucl Mater* **443** (2013) 497-501.
[20]M. Wirtz, J. Linke, G. Pintsuk, et al., *J Nucl Mater* **420** (2012) 218-221.
[21]Y. Z. Jia, W. Liu, B. Xu, et al., *Nucl Fusion* **55** (2015) 113015.
[22]G. De Temmerman, J. J. Zielinski, S. van Diepen, et al., *Nucl Fusion* **51** (2011) 073008.
[23]T. W. Morgan, T. M. de Kruif, H. J. van der Meiden, et al., *Plasma Phys Contr F* **56** (2014) 0950049.
[24]A. Herrmann, W. Junker, K. Gunther, et al., *Plasma Phys Contr F* **37** (1995) 17-29.
[25]M. Miyamoto, D. Nishijima, Y. Ueda, et al., *Nucl Fusion* **49** (2009) 650356.
[26]W. M. Shu, A. Kawasuso, Y. Miwa, et al., *Phys Scripta* **T128** (2007) 96.
[27]Y. Yuan, J. Du, M. Wirtz, et al., *Nucl Fusion* **56** (2016) 036021.
[28]V. K. Alimov, B. Tyburska-Pueschel, S. Lindig, et al., *J Nucl Mater* **420** (2012) 519-524.
[29]G. N. Luo, W. M. Shu, M. Nishi, *Fusion Eng Des* **81** (2006) 957-962.
[30]L. Wang, B. Wang, S. Li, et al., *Int. Journal of Refractory Metals and Hard Materials* **61** (2016) 61-66.
[31]J. W. Christian, *Metallurgical Transaction A* **14** (1983) 1237-1256.
[32]J. W. Davis, V. R. Barabash, A. Makhankov, et al., *J Nucl Mater* **258** (1998) 308-312.

Table.1 Conditions of stationary D plasma.

Fig.1 Surface temperature of samples exposed to stationary/pulsed plasma. (a) Temperature evolution during a shot; (b) temperature and heat flux distribution over the surface.

Fig.2 Surface morphology of exposure surfaces with different ΔT (scale bar is the same). (a) 320 K, (b) 360 K, (c) 400 K, (d) 500 K, (e) 600 K, and (f) 700 K.

Fig.3 Effect of ΔT on the surface morphology of different surfaces (scale bar is the same). (a)-(d) ΔT = 320 K, 400 K, 500 K, and 700 K, surface morphology of [001] surfaces; (e)-(h) ΔT = 320 K, 400 K, 500 K, and 700 K, surface morphology of [110] surfaces; (i)-(l) ΔT = 320 K, 400 K, 500 K, and 700 K, surface morphology of [111] surfaces.

Fig.4 Effect of ΔT on blistering of [001], [110] and [111] surfaces with BT = 650 K

Fig.5 Surface morphology and cross-section morphology of the tiny cracks on the surface. (a), (c) Surface morphology; (b), (d) Cross-section morphology; (e) Schematic diagram of micro cracks.

Fig.6 Surface morphology of exposure surfaces with different ΔT (scale bar is the same). (a) 200 K, (b) 240 K, (c) 300 K, (d) 400 K, (e) 550 K, and (f) 700 K.

Fig.7 Effect of ΔT on the surface morphology of different surfaces (scale bar is the same). (a)-(d) ΔT = 240 K, 400 K, 550 K, and 700 K, surface morphology of [001] surfaces; (e)-(h) ΔT = 240 K, 400 K, 550 K, and 700 K, surface morphology of [110] surfaces; (i)-(l) ΔT = 240 K, 400 K, 550 K, and 700 K, surface morphology of [111] surfaces.

Fig.8 Effect of ΔT on blistering of [001], [110] and [111] surfaces with BT=800 K.

Fig.9 Effects of BT and ΔT on surface modification.

Fig.10 Cracking on W surface exposed to pulsed plasma. (a) BT = 650 K, ΔT = 700 K; (b) BT = 800 K, ΔT = 700 K.

Table.1

Species	Flux density ($m^{-2}s^{-1}$)	Fluence (m^{-2})	Ion energy (eV)	Number of shots
D	$\sim 1\times10^{24}$	$\sim 1\times10^{26}$	~38	10

Fig.1

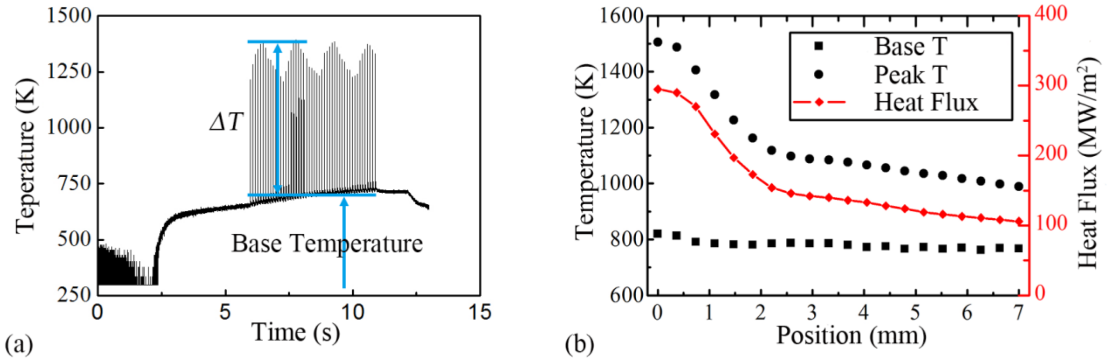

1500
1250
1000
750
500
250
Teperature (K)
0
5
10
15
Time (s)
ΔT
Base Temperature
(a)
1600
1400
1200
1000
800
600
Temperature (K)
0
1
2
3
4
5
6
7
Position (mm)
400
300
200
100
0
Heat Flux (MW/m²)
Base T
Peak T
Heat Flux
(b)

Fig.2

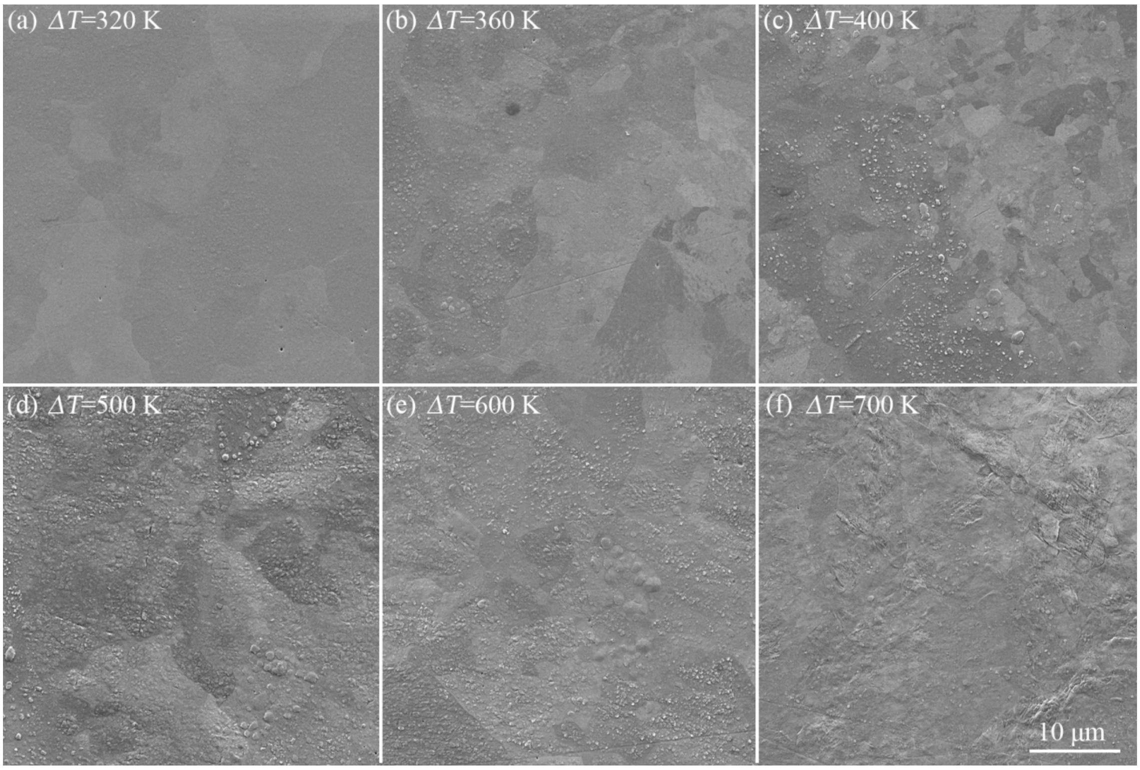

Fig.3

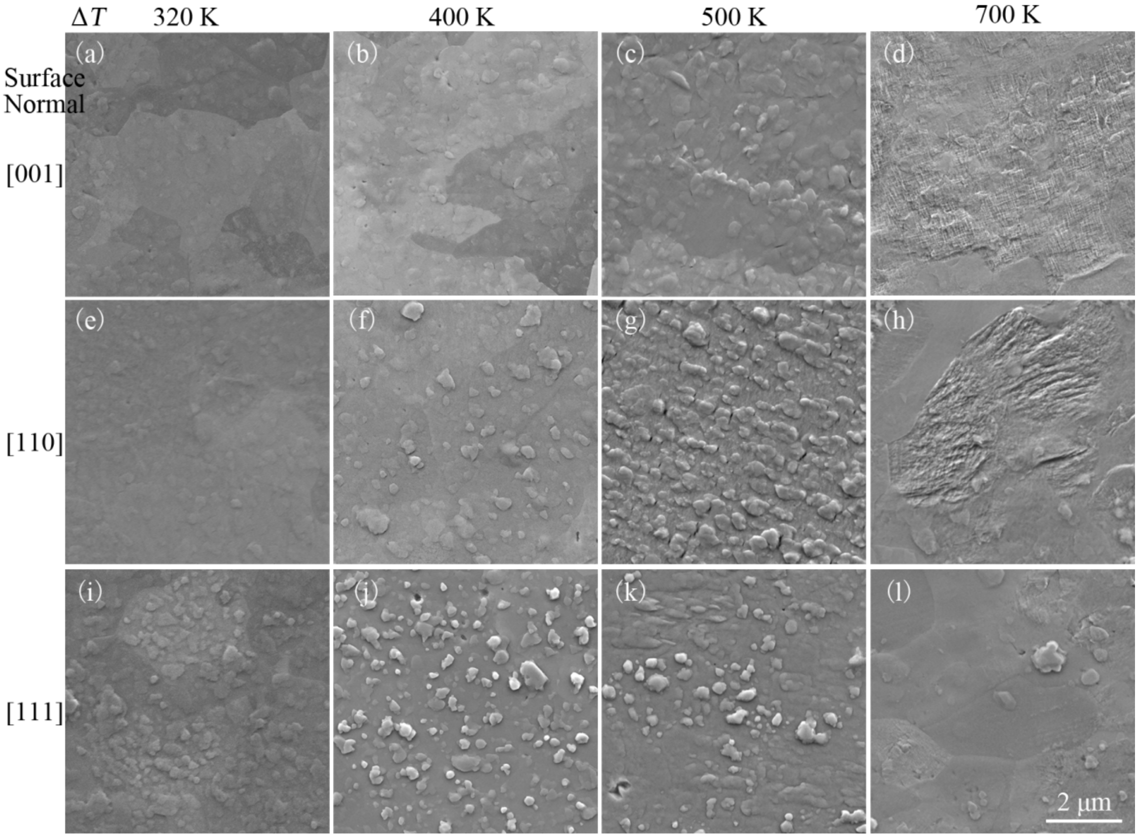

ΔT
320 K
400 K
500 K
700 K
Surface Normal
[001]
[110]
[111]
(a)
(b)
(c)
(d)
(e)
(f)
(g)
(h)
(i)
(j)
(k)
(l)
2 μm

Fig.4

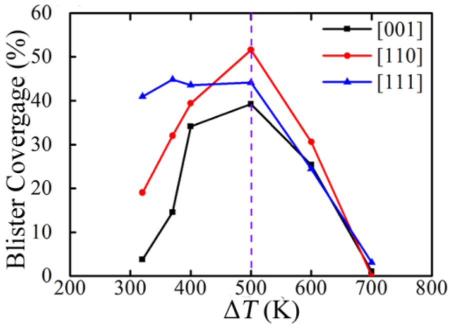

Blister Covergage (%)
0
10
20
30
40
50
60
200
300
400
500
600
700
800
ΔT (K)
[001]
[110]
[111]

Fig.5

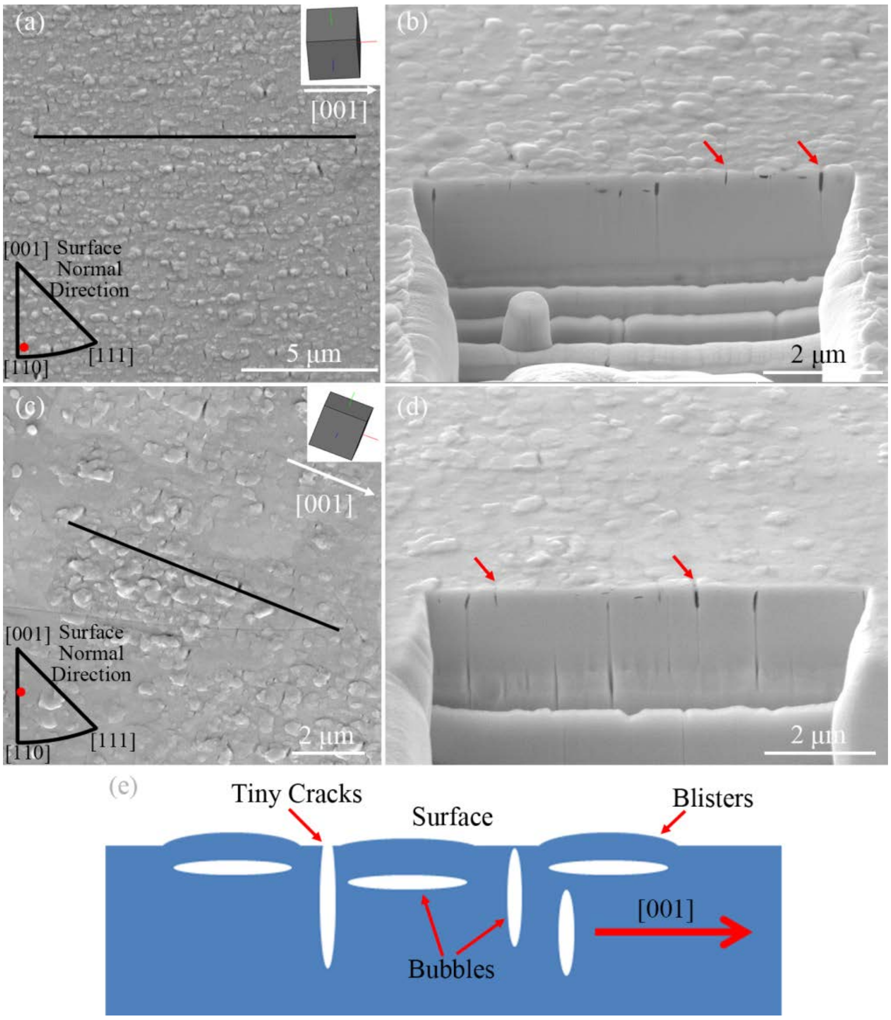

(a)
[001]
[001] Surface
Normal
Direction
[110]
[111]
5 μm
(b)
2 μm
(c)
[001]
[001] Surface
Normal
Direction
[110]
[111]
2 μm
(d)
2 μm
(e)
Tiny Cracks
Surface
Blisters
Bubbles
[001]

Fig.6

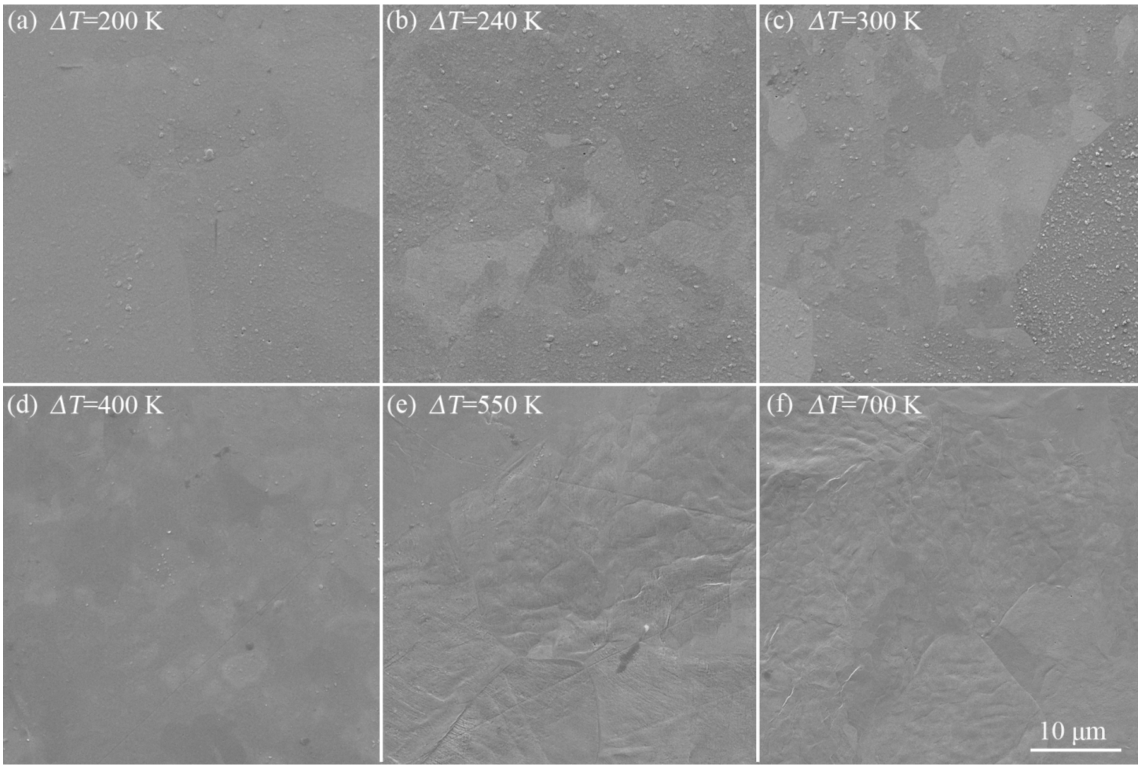
(a) ΔT=200 K
(b) ΔT=240 K
(c) ΔT=300 K
(d) ΔT=400 K
(e) ΔT=550 K
(f) ΔT=700 K
10 μm

Fig.7

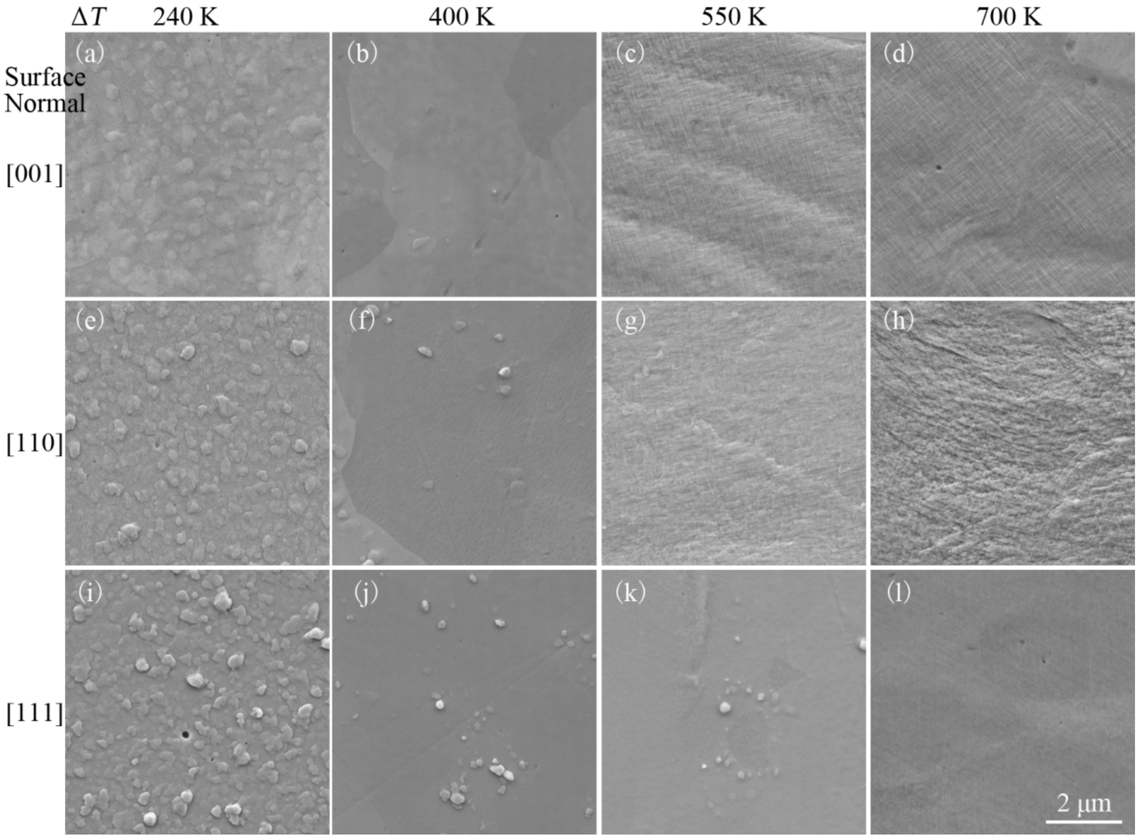

ΔT
240 K
400 K
550 K
700 K
Surface Normal
[001]
[110]
[111]
(a)
(b)
(c)
(d)
(e)
(f)
(g)
(h)
(i)
(j)
(k)
(l)
2 μm

Fig.8

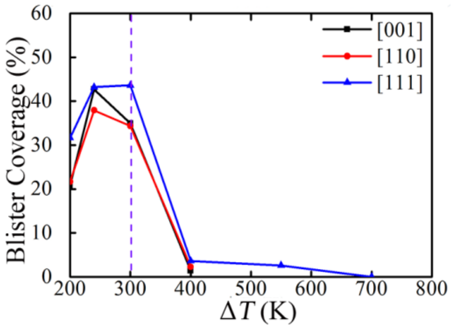
Blister Coverage (%)
0
10
20
30
40
50
60
200
300
400
500
600
700
800
ΔT (K)
[001]
[110]
[111]

Fig.9

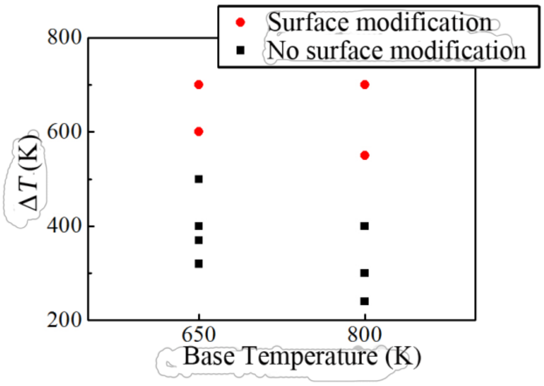

Surface modification
No surface modification
800
600
400
200
ΔT (K)
650
800
Base Temperature (K)

Fig.10